

## Mixed Convection in Horizontal Internally Finned Semicircular Ducts

A. M. Ben-Arous<sup>1</sup> and A. A. Busedra<sup>1</sup>

**Abstract:** The problem of combined free and forced convection in horizontal semicircular ducts (flat wall at the bottom) with radial internal fins is investigated from a numerical point of view. The wall of the duct is assumed to have a uniform heat input along the axial direction with a uniform peripheral wall temperature (H1). The analysis focuses on the case of hydrodynamically and thermally fully-developed laminar flow. The governing equations for the velocity and temperature are solved by using a control-volume-based finite-difference approach. The fluid flow and heat transfer characteristics are found to be dependent on the Grashof number, the fin length and the number of fins. It is also found that the heat transfer rate increases with the Grashof number and is more intense with respect to the case of finless semicircular ducts. The most remarkable outcome of the present study is that, for each number of fins an optimum fin length exists at which the Nusselt number attains a maximum.

**Keyword:** Laminar Mixed Convection, Semicircular Ducts.

### 1 Introduction

Internally finned ducts are used extensively in compact heat exchangers, solar collectors, and nuclear reactors. The semicircular duct is a classical example of ducts used in compact heat exchangers. It may be used also as a stand alone duct, because of the presence of a flat wall. Moreover, the additional surface provided by the internal fins can enhance the heat transfer. Some relevant literature on the subject is discussed in the following.

Dong and Ebdian (1995) have studied the effect

of radial internal fins on heat transfer and pressure drop for laminar fully developed mixed convection in vertical semicircular ducts with the H1 thermal boundary condition.

Prakash and Patankar (1981) studied the fully developed laminar mixed convection in a vertical tube with internal fins for the same thermal boundary condition. Mirza and Soliman (1985) obtained numerical solutions in horizontal tubes with two vertically oriented fins. Rustum and Soliman (1990) extended this analysis to a wide geometrical range in terms of fin lengths and number of fins. In both investigations, the presence of the fins was found to delay and suppress the free convection effects compared to finless tubes.

Laminar mixed convection in horizontal tubes with longitudinal internal fins was also investigated from an experimental point of view by Rustum and Soliman (1988). Their investigation included the pressure drop and heat transfer in the fully developed region.

Nandakumar, Masliyah and Law (1985) studied the fully developed mixed convection with the aforementioned H1 thermal boundary condition in a horizontal finless semicircular duct with the flat wall at the bottom. Lei and Trupp (1990a) studied the same problem with the flat wall on top. Their results showed that the values of Nusselt number for the flat wall on top are approximately the same as for the flat wall at the bottom.

Chinporoncharoenpong, Trupp and Soliman (1993) analyzed also the same problem by rotating the semicircular duct from 0° (the flat wall on top) to 180° (the flat wall at the bottom) with an incremental angle of 45°. They disclosed that, orienting the flat wall of the semicircular duct vertically 90° up to 135° gave the highest heat transfer rate among the other orientations. Busedra and El-Abeedy (2003) extended the

---

<sup>1</sup> Department of Mechanical Engineering, University of Garyounis, Benghazi, Libya

analysis of Chinporoncharoenpong et al. (1993) by inclining the semicircular duct at a fixed angle and a single value of the Reynolds number. They reported that, the effect of inclination on the orientation is important in heat transfer enhancement.

Busedra and Soliman (1999) elaborated some theoretical results for laminar fully developed mixed convection in heated semicircular ducts (with the flat wall in vertical position) with buoyancy-assisted and buoyancy-opposed inclinations using two thermal boundary conditions, H1 and H2 (axial uniform heat input combined with uniform circumferential wall heat flux). They investigated the effect of inclination on the axial velocity and temperature as well as the heat transfer and the pressure drop. They found that, the location of the maximum  $Nu$  at high  $Gr$  shifts to lower values of the inclination angle.

Busedra and Soliman (2000) have studied also the combined free and forced convection experimentally for laminar water flow in the entrance region of a semicircular duct with upward and downward inclinations within  $\pm 20^\circ$ . They oriented the flat wall in vertical position and compared their experimental results with their theoretical predictions. Recently, El-Hasadi, Busedra, and Rustum (2007) have analyzed numerically the laminar mixed convection in the entrance region of horizontal semicircular ducts with the flat wall on top. Their results, for  $Pr = 0.7$ , have provided local Nusselt number as well as the axial velocity and temperature fields at different axial locations. The present study deals with the case in which the flat wall of the semicircular duct is located at the bottom. We investigate the effect of radial internal fins on the heat transfer rate using the H1 thermal boundary condition.

### 1.0.1 Analysis and Modeling

The problem considered is that of fully developed laminar mixed convection in a horizontal semicircular duct with  $N$  radial fins, each with a length  $l$ . They are spaced around the circumference of the semicircular duct. The fins are also assumed to be of negligible thickness, and highly conductive. **Fig. 1** shows the cross section of the finned

semicircular duct.

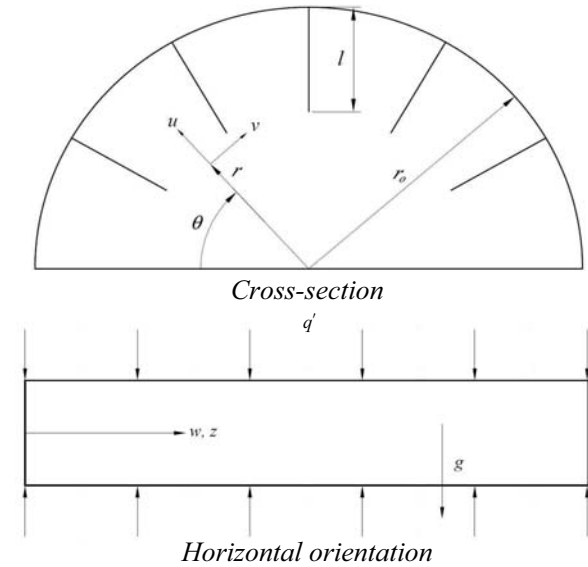


Figure 1: Geometry of a semicircular duct with internal fins

The fluid is assumed to be incompressible and Newtonian, and the flow is steady, laminar, and fully developed hydrodynamically and thermally. Viscous dissipation and axial heat diffusion are assumed to be negligible. Fluid properties are assumed to be constant, except for the variation of density in the buoyancy term, which varies with temperature according to Boussinesq approximation.

$$\rho = \rho_w (1 - \beta (t - t_w)) \quad (1)$$

The fluid pressure decomposition is given by Anderson, Tannehill and Pletcher (1984) as follows:

$$p(r, \theta, z) = p_1(z) + p_2(r, \theta) \quad (2)$$

where  $p_1$  is the cross-sectional average pressure, which is assumed to vary linearly in the  $z$ -direction, while  $p_2$  ( $p_2^* = p_2^+ \rho_w g r \sin \theta$ ) provides the driving force for the secondary flow within the cross-section. The problem dimensionless parameters are:

$$\left. \begin{aligned} R &= \frac{r}{r_0}, Z = \frac{z}{r_0}, U = \frac{ur_0}{v}, V = \frac{vr_0}{v}, \\ W &= \frac{w}{w_m}, L = \frac{l}{r_0}, f = D \frac{\partial p_1}{2\rho w_m^2}, \\ P_1 &= \frac{p_1 r_0}{\rho v w_m}, P_2 = \frac{p_2^* r_0^2}{\rho v^2}, T = \frac{t - t_w}{q' / (\frac{4}{\pi} k)}, \\ Re &= \frac{D w_m}{v}, Pr = \frac{\rho v C_p}{k}, Gr = \frac{g \beta q' r_0^3}{\frac{4}{\pi} k v^2} \end{aligned} \right\} \quad (3)$$

The governing equations can be written in dimensionless form as:

Continuity equation:

$$\frac{\partial(RU)}{\partial R} + \frac{\partial V}{\partial \theta} = 0 \quad (4)$$

Momentum equations:

*R*-direction:

$$U \frac{\partial U}{\partial R} + \frac{V}{R} \frac{\partial U}{\partial \theta} = -\frac{\partial P_2}{\partial R} + \nabla^2 U - \frac{2}{R^2} \frac{\partial V}{\partial \theta} - \frac{U}{R^2} + \frac{V^2}{R} + GrT \sin \theta \quad (5)$$

$\theta$ -direction:

$$\left( U \frac{\partial V}{\partial R} + \frac{V}{R} \frac{\partial V}{\partial \theta} \right) = -\frac{1}{R} \frac{\partial P_2}{\partial \theta} + \nabla^2 V + \frac{2}{R^2} \frac{\partial U}{\partial \theta} - \frac{V}{R^2} - \frac{UV}{R} + GrT \cos \theta \quad (6)$$

*Z*-direction:

$$U \frac{\partial W}{\partial R} + \frac{V}{R} \frac{\partial W}{\partial \theta} = \frac{1}{2} fRe + \frac{1}{R} \frac{\partial}{\partial R} \left( R \frac{\partial W}{\partial R} \right) + \frac{1}{R^2} \frac{\partial^2 W}{\partial \theta^2} \quad (7)$$

Energy equation

$$Pr \left( U \frac{\partial T}{\partial R} + \frac{V}{R} \frac{\partial T}{\partial \theta} \right) = \nabla^2 T - \left( \frac{2}{\pi} \right) W \quad (8)$$

The associated boundary conditions are given as:

$W = V = U = 0$  on the fins and on the walls

$T = 0$  on the walls

Where  $\nabla^2$  is:

$$\nabla^2 = \frac{1}{R} \frac{\partial}{\partial R} \left( R \frac{\partial}{\partial R} \right) + \frac{1}{R^2} \frac{\partial^2}{\partial \theta^2} \quad (9)$$

### 1.1 Parameter of Interest

The following definition of the Nusselt number,  $Nu$  is used in present study:

$$Nu = \frac{hD}{k} = \frac{\pi}{(\pi+2)} \left( \frac{1}{-T_b} \right) \quad (10)$$

In the above equation the diameter of the circular duct is used as the reference length. This definition makes it easier to compare results for finless and finned ducts.

### 1.2 Solution Technique

The dimensionless governing partial differential equations (Eqs. 4–8) have been discretized by using a finite control volume approach (Patankar (1980)), and a power law scheme has been used for the treatment of the convection and diffusion terms. The velocity-pressure coupling has been handled using the SIMPLER algorithm of Patankar (1980). A staggered grid has been used in the computations with uniform subdivisions in the *R* and  $\theta$  directions.

For given values of the input parameters *Pr* and *Gr*, computations have been started from an initial guess of the fields (*U*, *V*, *W*, *T*). Typically, the initial guess used was  $U = V = W = T = 0$  at all mesh points.

The discretized equations have been solved simultaneously for each radial line using the tridiagonal matrix algorithm [TDMA], and the domain has been covered by sweeping line by line in the angular direction.

At the end of each iteration, a correction procedure has been applied to *W*, using the conservation of mass, in order to ensure that the mean value of the dimensionless velocity,  $W_m$  is equal to 1. This correction procedure follows the method outlined by Patankar and Spalding (1972): the converged velocity profile must satisfy the condition:

$$\int_0^\pi \int_0^1 WRdRd\theta = \frac{\pi}{2} \quad (11)$$

The following convergence criterion for the three velocity components and the temperature at all grid points has been used:

$$\left| \frac{\phi_{new} - \phi_{old}}{\phi_{new}} \right| \leq 10^{-6} \quad (12)$$

It has been found that a selected grid size of  $61 \times 141$  (*R*  $\times$   $\theta$ ) for finless semicircular ducts is capable of producing  $Nu_o$  value of 6.689 and  $(fRe)_o$  value of 42.218 for pure forced convection. These values show that excellent agreement has been reached between the present study and the exact values of Lei and Trupp (1990b) ( $Nu_o = 6.690$  and  $(fRe)_o = 42.232$ ). In generating the final

Table 1: Comparison of  $Nu_o$  and  $(fRe)_o$  for forced convection

Number of fins	Fin Length	$Nu_o$		$(fRe)_o$	
		Present	Dong and Ebadian (1995)	Present	Dong and Ebadian (1995)
3	0.2	7.571	7.531	53.022	53.345
	0.4	12.177	12.171	87.985	87.943
	0.6	25.040	24.816	142.06	141.762

results for semicircular ducts with radial internal fins, a selected mesh size ( $61 \times 141$ ) for  $N = 3$  and 9 was considered. The accuracy of the results was also compared with Dong and Ebadian (1995) for the case of fully developed forced convection in case of  $N = 3$  with different fin lengths, as shown in **Tab. 1**

## 2 Results and Discussion

A single value of Prandtl number,  $Pr = 7$  has been used in all computations with  $Gr$  up to  $10^6$ . The secondary flow patterns and temperature profiles as well as  $fRe$  and  $Nu$  have been examined.

### 2.1 Secondary Flow Pattern

Figure 2 represents the secondary flow pattern for  $N = 3$  and  $N = 9$  with fin lengths of 0.2 and 0.6.

**Fig. 2-a** shows the secondary flow pattern consists of two identical counter rotating secondary flow cells appearing in the lower corners of the semicircular duct.

The fluid in the upper central part moves upward around the tip of the lower two fins and then along the curved wall towards the upper central fin.

The trend does not change as the number of fins increases to  $N = 9$ , as shown in **Fig. 2-b**. However, increasing the fin length to  $L = 0.6$  causes a complicated secondary flow pattern, as shown in **Figs. 2-c** and **2-d**.

### 2.2 Temperature Distribution

Figure 3 shows the temperature distribution.

**Fig. 3-a**, with short fins and  $N = 3$ , shows that the cooler fluid core shifts to the lower part of the duct. As a result, an important temperature gradient is observed there. Such a gradient leads to a much more effective heat transfer with respect to

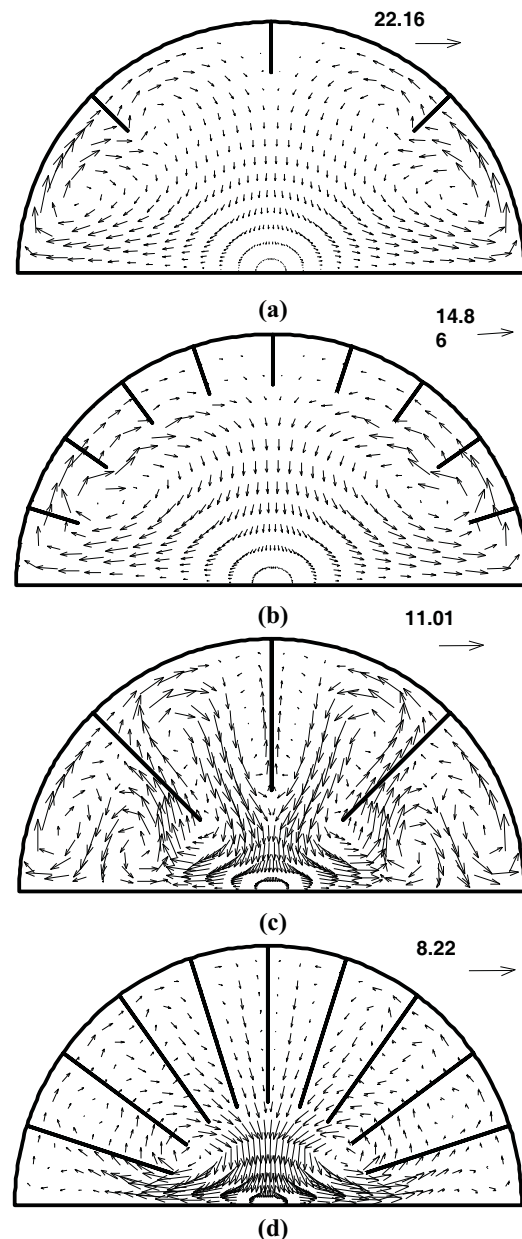


Figure 2: Secondary flow pattern for  $L = 0.2$  and  $0.6$  with  $N = 3$  and 9 at  $Gr = 1 \times 10^6$

heat transfer established in the upper part. The underlying reason is that, the circulation of the secondary flow is more intense in the lower part than in the upper part. A similar trend can be seen in **Fig. 3-b** for  $N = 9$  with  $L = 0.2$ .

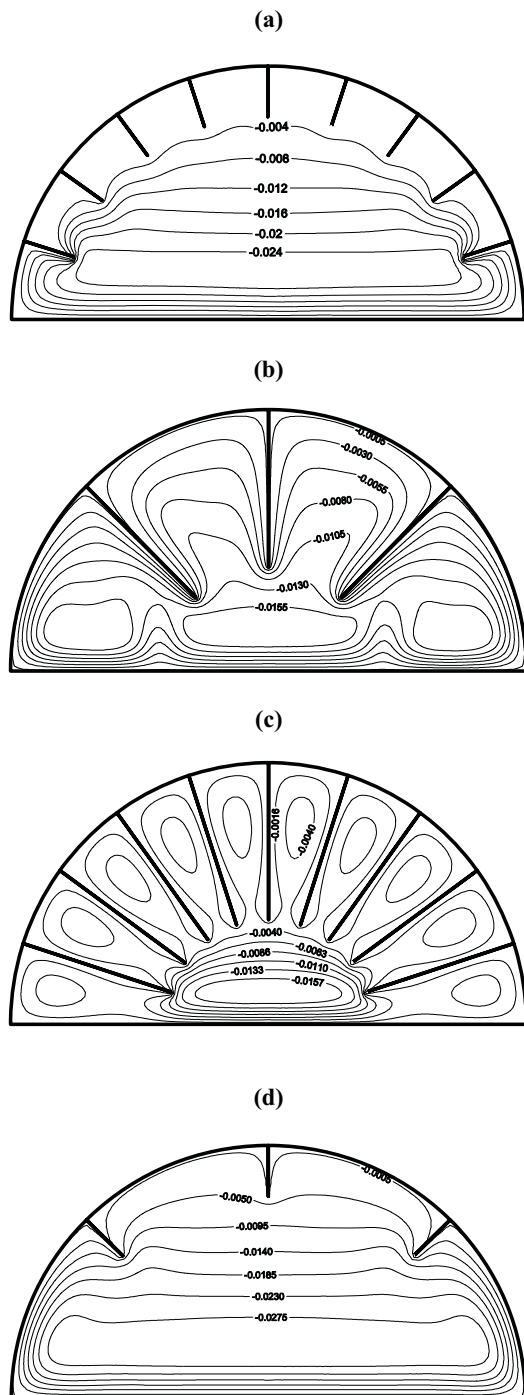


Figure 3: Temperature distribution for  $L = 0.2$  and  $0.6$  with  $N = 3$  and  $9$  at  $Gr = 1 \times 10^6$

At the same Grashof number (e.g;  $Gr = 1 \times 10^6$ ) **Figs. 3-c**, and **3-d** show the effect of the secondary flow on the temperature distribution in the semicircular duct with long fins. It can be seen that the cooler fluid core is split in several parts by the fins. In particular, **Fig. 3-c** shows that the temperature values are approximately the same in the lower corners and in the two upper bays. A similar behavior can be seen in **Fig. 3-d** with  $N = 9$ .

### 2.3 Friction Factor and Nusselt number

The ratio  $fRe/(fRe)_o$ , where  $(fRe)_o$  corresponds to pure forced convection for the same geometry is presented in **Fig. 4** for  $N = 3$  and  $9$  with different lengths ( $L = 0.2$  and  $0.6$ ). These results show that  $fRe/(fRe)_o$  remains close to unity up to a critical  $Gr$  beyond which  $fRe/(fRe)_o$  increases slightly with increasing  $Gr$ . This critical  $Gr$  increases as  $L$  increases and  $fRe/(fRe)_o$  decreases with increasing  $L$  at any given  $Gr$ .

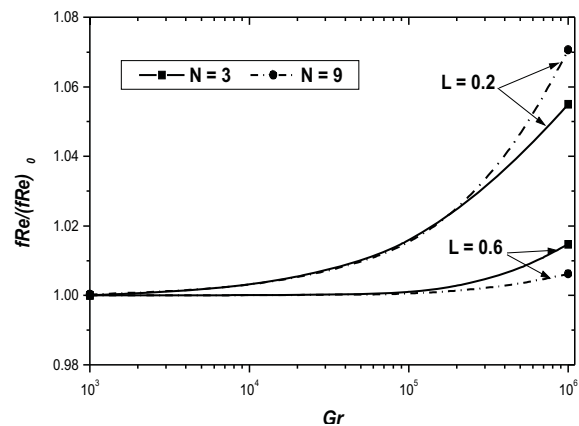


Figure 4: The effect of  $Gr$  on  $fRe/(fRe)_o$  for  $N = 3$  and  $9$  with  $L = 0.2$  and  $0.6$

Figure 5 shows the variation of  $Nu/Nu_o$  with  $Gr$ , where  $Nu_o$  corresponds to pure forced convection for the same geometry. The prevailing trends are similar to those illustrated for the friction factor in **Fig. 4**, but the amount of increase in  $Nu/Nu_o$  values is much larger. This is due to the influence of free convection currents on the temperature distribution.

Moreover, at any given value of  $Gr$ , shorter fins have higher values of  $Nu/Nu_o$  than the longer

fins. It is worth highlighting that the way by which variations in  $N$  and  $L$  influence  $Nu/Nu_o$  and  $fRe/(fRe)_o$  are consistent with the results of Rustum and Soliman (1990).

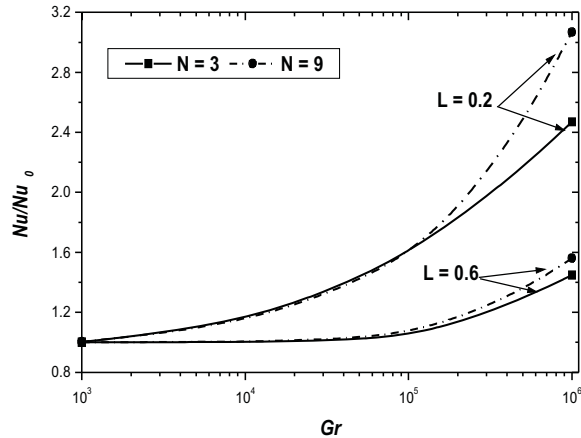


Figure 5: The effect of  $Gr$  on  $Nu/Nu_o$  for  $N = 3$  and  $9$  with  $L = 0.2$  and  $0.6$

The ratio  $Nu/Nu_o$  as a function of all considered values of  $N$  and  $L$  is presented in **Fig. 6**.

For each number of fins, an optimum fin length exists at which  $Nu/Nu_o$  reaches a maximum. The optimum fin length increases as the number of fins increases.

A pronounced enhancement of heat transfer can be obtained by using shorter fins. The Values of  $Nu/Nu_o$  with shorter fins ( $L = 0.2$ ), for  $Gr = 1 \times 10^6$ , as compared with finless semicircular ducts of Chinporoncharoenpong, Trupp and Soliman (1993) are higher by 6.3% and, 32% for  $N = 3$ , and  $9$  respectively. Thus **Fig. 6** ascertains that increasing the fin length in these cases is not necessary for heat transfer enhancement.

### 3 Conclusions

Fully developed laminar mixed convection in horizontal semicircular ducts (flat wall at the bottom) with radial internal fins and with the well-known H1 thermal boundary condition has been investigated.

The effect of the number of fins and fin length on the heat transfer has been clarified. The results show that the semicircular duct geometry has a

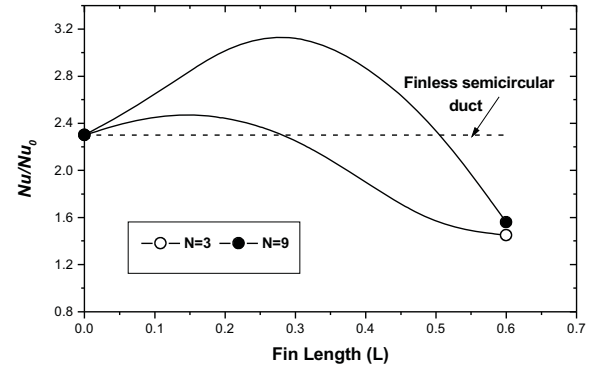


Figure 6: Values of  $Nu/Nu_o$  for  $N = 3$  and  $9$  with different lengths at  $Gr = 1 \times 10^6$

strong influence on the secondary flow currents, which is in turn reflected on the temperature distribution and heat transfer rate.

Remarkably, at  $Gr = 1 \times 10^6$  with longer fins the secondary flow is suppressed in the bays delimited by the fins.

The circulation exhibits a larger magnitude in the lower part of the section with respect to the upper part. As a result, a considerable temperature gradient is established there. Such a gradient is responsible for heat transfer much more intense in the lower region than in the upper region.

The ratio  $Nu/Nu_o$  has been found to increase with  $Gr$  in all cases. For each number of fins, an optimum fin length exists at which  $Nu/Nu_o$  reaches a maximum. By comparing the results of finless semicircular ducts with those for finned ducts, it is evident that the heat transfer is enhanced by using short fins (this means that increasing the fin length is may be regarded as not necessary for heat transfer enhancement).

### Nomenclature

- $C_p$  specific heat, J/kg k
- $D$  diameter of the semicircular duct ( $= 2r_o$ ), m
- $f$  fanning friction factor
- $g$  gravitational acceleration,  $m/s^2$
- $Gr$  Grashof number
- $h$  average heat transfer coefficient,  $W/m^2 k$
- $k$  thermal conductivity of the fluid,  $W/m k$
- $l$  fin length, m

$L$  dimensionless fin length  
 $N$  number of fins  
 $Nu$  average Nusselt number  
 $P$  Pressure  $N/m^2$   
 $p_1$  cross-sectional average pressure,  $N/m^2$   
 $p_2$  cross sectional excess pressure,  $N/m^2$   
 $P_1$  dimensionless cross-sectional average pressure  
 $P_2$  dimensionless cross-sectional excess pressure  
 $Pr$  Prandtl number  
 $q'$  rate of heat input per unit length,  $W/m$   
 $r$  radial coordinate,  $m$   
 $r_o$  radius of circular wall,  $m$   
 $R$  dimensionless radial coordinate  
 $Re$  Reynolds number  
 $t$  temperature,  $K$   
 $T$  dimensionless temperature  
 $T_b$  dimensionless bulk temperature  
 $u$  radial velocity,  $m/s$   
 $U$  dimensionless radial velocity  
 $v$  angular velocity,  $m/s$   
 $V$  dimensionless angular velocity  
 $w$  axial velocity,  $m/s$   
 $W$  dimensionless axial velocity  
 $z$  axial coordinate,  $m$   
 $Z$  dimensionless axial coordinate

#### Greek Symbols

$\beta$  coefficient of thermal expansion,  $K^{-1}$   
 $\theta$  angular coordinate, radians  
 $\nu$  kinematic viscosity,  $m^2/s$   
 $\rho$  Density of the fluid,  $kg/m^3$

#### Subscripts

$m$  mean value  
 $o$  corresponding to  $Gr = 0$   
 $w$  at the wall

#### References

- Anderson D. A.; Tannehill J. C.; Pletcher R. H.** (1984): Computational Fluid Mechanics and Heat Transfer. *McGraw-Hill, New York*.
- Busedra A. A.; El-abeedy E. A.** (2003): Effect of Orientation on Laminar Mixed Convection for Inclined Semicircular Ducts, *Proceedings of the 3<sup>rd</sup> Int. Conf. for Energy and Environment, Brack, Libya*.
- Busedra A. A.; Soliman H. M.** (1999): Analysis of Laminar Mixed Convection in Inclined Semicircular Ducts Under Buoyancy Assisted and Opposed Conditions, *Num. Heat Transfer, Part A*, vol. 36, pp. 527-544.
- Busedra A. A.; Soliman H. M.** (2000): Experimental Investigation of Laminar Mixed Convection in an Inclined Semicircular Duct Under Buoyancy Assisted and Opposed Conditions, *Int. J. Heat Mass Transfer*, vol. 43, pp. 1103-1111.
- Chinporcharoenpong C.; Trupp A. C.; Soliman H. M.** (1993): Effect of Gravitational force Orientation on Laminar Mixed Convection for a Horizontal Semicircular Duct, *Proc. 3<sup>rd</sup> World Conf. On Experimental Heat Transfer, Fluid Mechanics and Thermodynamics*, vol. 109, pp. 131-137.
- Dong, Z. F.; Ebadian, M. A.** (1995): Analysis of Combined Natural and Forced Convection in Vertical Semicircular Ducts With Radial Internal Fins, *Num. Heat Transfer, Part A*, vol. 3, pp. 341-355.
- El-Hasadi Y. M. F.; Busedra A. A.; Rustum I. M.** (2007): Laminar Mixed Convection in the Entrance Region of Horizontal Semicircular Ducts with the Flat wall on Top, *ASME J Heat Transfer*, vol. 129, pp. 1203-1211.
- Lei Q.; Trupp A. C.** (1990a): Predictions of Laminar Mixed Convection in a Horizontal Semicircular Duct, *6<sup>th</sup> Miami Int. Symposium on Heat and Mass Transfer*, vol. 4, pp. 10-12.
- Lei Q.; Trupp A. C.** (1990b): Forced Convection of Thermally Developed Laminar Flow in Circular Sector Ducts, *Int. J. Heat Mass Transfer*, vol. 33, pp. 1675-1683.
- Mirza S.; Soliman, H. M.** (1985): The Influence of Internal Fins on Mixed Convection Inside Horizontal Tubes, *Int, Commune. Heat Transfer*, vol. 12, pp. 191-200.
- Nandakumar K.; Masliyah J. H.; Law H. S.** (1985): Bifurcation in Steady Laminar Mixed Convection Flow in Horizontal Ducts, *J. Fluid Mech.*, vol. 152, pp. 145-161.
- Parakash, C.; Patankar, S. V.** (1981): Combined Free and Forced Convection in Vertical tubes With Radial Internal Fins, *Trans, ASME*,

vol. 103, pp. 566-572.

**Patankar S. V.** (1980): Numerical Heat Transfer and Fluid flow, *Mc-Graw Hill, New York*.

**Patankar S. V.; Spalding D. B.** (1972): A Calculation Procedure for Heat, Mass and Momentum Transfer in Three-Dimensional Parabolic Flows, *Int. J. Heat Mass Transfer*, vol. 15, pp. 1787-1806.

**Rustum I. M.; and Soliman H. M.** (1988): Experimental Investigation of Laminar Mixed Convection in Tubes With Longitudinal Internal Fins, *ASME J. Heat Transfer*, vol. 110, pp. 366-372.

**Rustum I. M.; and Soliman H. M.** (1990): Numerical Analysis of Laminar Mixed Convection in Horizontal Internally Finned Tubes, *Int. J. Heat Mass Transfer*, vol. 33, pp. 1485-1496.